



# Three-Dimensional Noncoaxial Plasticity Modeling of Shear Band Formation in Geomaterials

J. G. Qian<sup>1</sup>; J. Yang, M.ASCE<sup>2</sup>; and M. S. Huang<sup>3</sup>

**Abstract:** Accurate prediction of shear band formation in geomaterials is crucial in the solution of various stability problems in geotechnical engineering. The initiation of shear band is strongly dependent on the constitutive description of the prelocalization homogeneous deformation. Conventional plasticity models assume that coaxiality exists between the directions of principal stresses and the directions of plastic strain increments. Accumulating evidence has however shown that this assumption is not appropriate. In this paper, a noncoaxial constitutive modeling platform is presented in a general three-dimensional stress space. It is shown that the classical vertex-like structure, which has been widely adopted to describe the noncoaxial constitutive response, only represents the two-dimensional condition. Examples are presented to demonstrate the capability of the modeling platform in capturing the initiation and orientation of shear band in a granular soil. The significance of the noncoaxiality effects is illustrated by comparisons of the predictions produced by coaxial and noncoaxial (both two-dimensional and three-dimensional) plasticity models.

**DOI:** 10.1061/(ASCE)0733-9399(2008)134:4(322)

**CE Database subject headings:** Bifurcations; Constitutive models; Three-dimensional models; Geomaterials; Plasticity.

## Introduction

Strain localization is a typical feature of geomaterials such as soils and rocks when they undergo nonhomogeneous deformation. The zone of localized deformation is commonly referred to as shear band or simply rupture plane. Localized deformation is generally followed by reduction in the overall strength of the material as the loading proceeds, suggesting the importance of accurately predicting shear band formation in geotechnical applications. Over the past decades there have been numerous experimental investigations into the strain localization of granular soils (e.g., Arthur et al. 1977; Desrues et al. 1985; Hammad 1991; Han and Drescher 1993; Chu et al. 1996; Mooney et al. 1998; Wang and Lade 2000; Yamamuro and Shapiro 2002; Alshibli et al. 2003). These experimental works have revealed that the shear band formation is influenced by a number of factors, including the porosity of the material, inherent and stress-induced anisotropy of the material, particle size and shape of the material, and the level of confining stress.

It should be emphasized that the overall material response observed in the laboratory is a result of various micromechanical processes such as particle rolling and sliding in granular soils and microcracking in brittle rocks. Ideally, a localization model should capture all of these processes at the microscopic level.

However, limitations with laboratory testing capabilities and mathematical modeling techniques render the microscopic description of the constitutive behavior very difficult. The macroscopic approach involving the theory of plasticity is usually adopted (Vardoulakis 1980; Vermeer 1982; Desrues et al. 1985; Ottosen and Runesson 1991; Bardet 1991). In a standard plasticity model, the directions of principal stresses and the directions of plastic strain increments are implicitly assumed to be coaxial. However, accumulating evidence from experiments has shown that the plastic strain rate is dependent not only on the current state of stress but also on the current stress rate. In particular, a permanent plastic deformation can even accumulate when principal stresses rotate without any change in amplitude (Ishihara and Towhata 1983; Pradel et al. 1990; Gutierrez et al. 1991; Yang et al. 2007). These observations suggest the importance of accounting for the noncoaxiality between the principal directions of the stress and plastic strain increment in constitutive modeling.

Several theories have been developed to describe the noncoaxial behavior of engineering materials. Of the most notable is that by Rudnicki and Rice (1975), who pointed out that the bifurcation analysis with a constitutive formulation involving a smooth yield surface tended to predict excessively negative values of the tangent modulus for the onset of localization. To tackle this problem, they added a vertex-like structure to an isotropic hardening constitutive model to facilitate inception of shear band in the strain hardening region. The introduction of a vertex-like structure leads directly to a noncoaxial plastic flow rule and the effect of softened tangent modulus in the constitutive model. In line with this concept, several constitutive models for granular materials were revised to include noncoaxiality in the study of strain localization in soils (Vardoulakis and Graf 1985; Papamichos and Vardoulakis 1995). Results have shown that the noncoaxial models generally provide more reasonable predictions of shear band formation than the coaxial models.

The classical “vertex-like structure” proposed by Rudnicki and Rice (1975), as will be elaborated on later, does not represent the noncoaxial constitutive response in a general three-dimensional

<sup>1</sup>Dept. of Geotechnical Engineering, Tongji Univ., Shanghai, China.

<sup>2</sup>Dept. of Civil Engineering, Univ. of Hong Kong, Hong Kong, China (corresponding author). E-mail: junyang@hku.hk

<sup>3</sup>Dept. of Geotechnical Engineering, Tongji Univ., Shanghai, China.

Note. Associate Editor: George Z. Voyiadjis. Discussion open until September 1, 2008. Separate discussions must be submitted for individual papers. To extend the closing date by one month, a written request must be filed with the ASCE Managing Editor. The manuscript for this paper was submitted for review and possible publication on November 22, 2006; approved on August 17, 2007. This paper is part of the *Journal of Engineering Mechanics*, Vol. 134, No. 4, April 1, 2008. ©ASCE, ISSN 0733-9399/2008/4-322-329/\$25.00.

tensorial space. Keeping this in mind, this paper presents a noncoaxial plasticity modeling platform in a general three-dimensional tensorial space. The effects of noncoaxiality on shear band formation in granular soils are investigated by comparison of the predictions from coaxial and noncoaxial models (in both two- and three-dimensional spaces) with experimental observations. Stress probe tests are also conducted in the three-dimensional noncoaxial deviatoric stress space to show the effects of noncoaxiality.

## Coaxial and Noncoaxial Flow Theories

### Coaxial Flow Rule

In the theory of plasticity, coaxiality is referred to as the coincidence between the principal directions of the stress,  $\sigma_{ij}$ , and the rate of plastic deformation,  $\dot{\varepsilon}_{ij}^p$ . This condition can be expressed as

$$\dot{\varepsilon}_{ik}^p \sigma_{kj} = \sigma_{ik} \dot{\varepsilon}_{kj}^p \quad (1)$$

In a standard plasticity model, the plastic potential function,  $Q$ , is defined as a function of three stress invariants, i.e.,  $Q=Q(I_1, J_2, J_3)$ , where  $I_1$ =first invariant of the stress tensor,  $\sigma_{ij}$ ; and  $J_2, J_3$ =second and third invariants of the deviatoric stress tensor,  $s_{ij}$ . The three invariants are given as follows:

$$I_1 = \sigma_{ii}, \quad J_2 = \frac{1}{2}s_{ij}s_{ij}, \quad J_3 = \frac{1}{3}s_{ij}s_{jk}s_{ki} \quad (2)$$

The rate of plastic deformation is then given by

$$\dot{\varepsilon}_{ij}^p = \dot{\lambda} \frac{\partial Q}{\partial \sigma_{ij}} = \dot{\lambda} \left( \frac{\partial Q}{\partial I_1} \frac{\partial I_1}{\partial \sigma_{ij}} + \frac{\partial Q}{\partial J_2} \frac{\partial J_2}{\partial \sigma_{ij}} + \frac{\partial Q}{\partial J_3} \frac{\partial J_3}{\partial \sigma_{ij}} \right) \quad (3)$$

where  $\dot{\lambda}$ =non-negative scalar that varies during the plastic loading history. Eq. (3) can be rewritten in the following form

$$\dot{\varepsilon}_{ij}^p = \dot{\lambda} (a_0 \delta_{ij} + a_1 s_{ij} + a_2 S_{ij}) \quad (4)$$

where  $\delta_{ij}$ =Kronecker delta, and  $S_{ij}$  is given by

$$S_{ij} = s_{ik}s_{kj} - \frac{2}{3}J_2\delta_{ij} - \frac{3}{2}\frac{J_3}{J_2}s_{ij} \quad (5)$$

It is evident that the three coefficients,  $a_0, a_1$ , and  $a_2$ =functions of the stress invariants, i.e.

$$a_0 = \frac{\partial Q}{\partial I_1}, \quad a_1 = \frac{\partial Q}{\partial J_2} + \frac{3}{2}\frac{\partial Q}{\partial J_3}\frac{J_3}{J_2}, \quad a_2 = \frac{\partial Q}{\partial J_3} \quad (6)$$

Note that  $\delta_{ij}$ =isotropic tensor and the stress tensor  $s_{ij}$  shares the same principal directions with the tensor  $S_{ij}$ . This implies that the standard plasticity model assumes an inherent coaxiality between principal directions of the stress and the plastic deformation rate. For purposes of clarity, Eq. (4) can be rewritten in the following form

$$\dot{\varepsilon}_{ij}^{cp} = \delta_{ij}\dot{\varepsilon}_{kk}^{cp} + \dot{\varepsilon}_{ij}^{cp} \quad (7)$$

where the superscript  $c$  stands for coaxiality;  $\dot{\varepsilon}_{kk}^{cp}$  represents the volumetric plastic strain rate; and  $\dot{\varepsilon}_{ij}^{cp}$  represents the deviatoric plastic strain rate. Further, the deviatoric plastic strain rate  $\dot{\varepsilon}_{ij}^{cp}$  is decomposed into two components: one is related to  $s_{ij}$  and the other is related to  $S_{ij}$ .

Now, consider a special case in which the plastic potential is independent of the third stress invariant, i.e., a two-dimensional case. The deviatoric plastic strain rate  $\dot{\varepsilon}_{ij}^{cp}$  can be given as

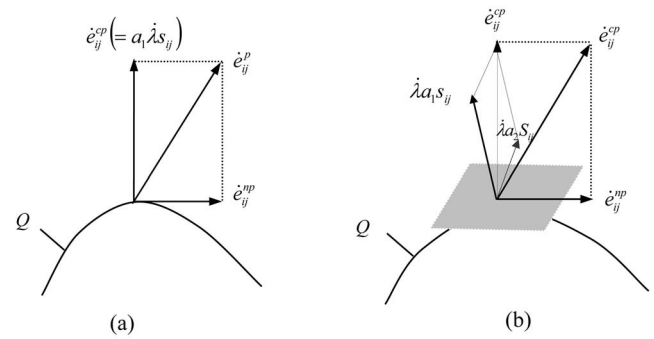


Fig. 1. Schematics of definition of  $\dot{\varepsilon}_{ij}^{np}$  in deviatoric stress space: (a) two-dimensional space; (b) three-dimensional space

$$\dot{\varepsilon}_{ij}^{cp} = a_1 \dot{\lambda} s_{ij} \quad (8)$$

Clearly, the above expression indicates that the rate of deviatoric plastic strain is always coaxial with  $\lambda a_1 s_{ij}$  if the third stress invariant is neglected.

### Noncoaxial Flow Rule in Deviatoric Stress Space

As mentioned earlier, there is increasing experimental evidence showing that the plastic strain increment is dependent not only on the current state of stress but also on the stress rate. In other words, there exists an incremental nonlinear plastic response or noncoaxial response. The yield vertex theory proposed by Rudnicki and Rice (1975) has been widely accepted in tackling the problem of noncoaxiality. In the yield vertex theory, the rate of noncoaxial plastic deformation,  $\dot{\varepsilon}_{ij}^{np}$ , is assumed to be linearly dependent on the noncoaxial stress rate,  $\hat{s}_{ij}^n$ , i.e.

$$\dot{\varepsilon}_{ij}^{np} = \dot{\varepsilon}_{ij}^{np} = \frac{1}{H_t} \hat{s}_{ij}^n \quad (9)$$

where the superscript  $n$  represents noncoaxiality; and  $H_t$  denotes the plastic modulus governing the response to the stress rate tangential to the yield surface,  $\hat{s}_{ij}^n$ , which is given by

$$\hat{s}_{ij}^n = \left( \hat{s}_{ij} - \frac{\hat{s}_{kl}s_{kl}}{s_{mn}s_{mn}} s_{ij} \right) \quad (10)$$

Note that an assumption is included in Eq. (9) that the noncoaxial plastic strain rate consists only of the deviatoric part. Also note that  $\dot{\varepsilon}_{ij}^{np}$  is orthogonal to  $\dot{\varepsilon}_{ij}^{cp}$ , because  $\hat{s}_{ij}^n$  is always orthogonal to  $s_{ij}, S_{ij}$ , and  $\delta_{ij}$ . As a result, the relationship expressed in Eq. (9) only describes the noncoaxial deformation in a two-dimensional deviatoric stress space, as illustrated in Fig. 1(a), but is not valid in a three-dimensional tensorial space  $\delta_{ij}-s_{ij}-S_{ij}$  as shown in Fig. 1(b). This notion is elaborated on below.

Assuming that the stress rate  $\hat{s}_{ij}$  is proportional to  $S_{ij}$  and equal to  $\dot{\lambda} S_{ij}$  ( $\dot{\lambda} \neq 0$ ), the noncoaxial plastic strain rate can be determined from Eq. (10) as

$$\dot{\varepsilon}_{ij}^{np} = \frac{1}{H_t} \left( \dot{\lambda} S_{ij} - \frac{\dot{\lambda} S_{kl}s_{kl}}{s_{mn}s_{mn}} s_{ij} \right) = \frac{1}{H_t} \dot{\lambda} S_{ij} \quad (11)$$

The above expression implies that the “noncoaxial” plastic strain rate is actually coaxial with the stress  $S_{ij}$  in the three-dimensional tensorial space.

In order to model the noncoaxial behavior in the three-dimensional space, one should formulate the noncoaxial strain

rate in such a manner that it is independent of the tensorial plan  $s_{ij}-S_{ij}$ . Here, we propose that the rate of noncoaxial stress is formulated in the form as follows:

$$\hat{s}_{ij}^n = \hat{s}_{ij} - \frac{\hat{s}_{kl}S_{kl}}{s_{mn}S_{mn}}s_{ij} - \frac{\hat{s}_{kl}S_{kl}}{S_{mn}S_{mn}}S_{ij} \quad (12)$$

It can be shown that  $\hat{s}_{ij}^n$  defined by Eq. (12) is a component tensor of  $\hat{s}_{ij}$ , and is orthogonal to  $\delta_{ij}$ ,  $s_{ij}$ , and  $S_{ij}$ , i.e.

$$\hat{s}_{ij}^n \delta_{ij} = 0, \quad \hat{s}_{ij}^n s_{ij} = 0, \quad \hat{s}_{ij}^n S_{ij} = 0 \quad (13)$$

Recalling that  $S_{ij}$  is dependent on the third stress invariant, Eq. (12) can be reduced to the one given by Rundnicki and Rice (1975) for the two-dimensional case where the third stress invariant is not involved.

### Elastic-Plastic Stiffness Incorporating Noncoaxiality

In this section, we will establish the elastic-plastic stiffness tensor incorporating noncoaxiality in the three-dimensional tensorial space. Based on the preceding discussion, the noncoaxial strain rate can be given as

$$\dot{\epsilon}_{ij}^{np} = \dot{\epsilon}_{ij}^{cp} = \frac{1}{H_t} \left( \hat{s}_{ij} - \frac{\hat{s}_{kl}S_{kl}}{s_{pq}S_{pq}}s_{ij} - \frac{\hat{s}_{kl}S_{kl}}{S_{pq}S_{pq}}S_{ij} \right) \quad (14)$$

Denote that

$$\dot{\epsilon}_{ij}^{np} = \dot{\epsilon}_{ij}^{cp} = C_{ijkl}^{np} \hat{\sigma}_{kl} \quad (15)$$

where  $C_{ijkl}^{np}$ =noncoaxial compliance tensor; and  $\hat{\sigma}_{kl}$ =stress rate. From Eqs. (14) and (15) we have

$$C_{ijkl}^{np} = \frac{1}{H_t} \left( \frac{\delta_{ik}\delta_{jl} + \delta_{il}\delta_{jk}}{2} - \frac{\delta_{kl}\delta_{ij}}{\delta_{mn}\delta_{mn}} - \frac{s_{ij}S_{kl}}{s_{mn}S_{mn}} - \frac{S_{ij}S_{kl}}{S_{mn}S_{mn}} \right) \quad (16)$$

Note that  $C_{ijkl}^{np}$  has the property of symmetry:  $C_{ijkl}^{np} = C_{klij}^{np} = C_{jilk}^{np} = C_{ijlk}^{np}$ .

When the yield function is independent of the third stress invariant, Eq. (16) can be simplified as

$$C_{ijkl}^{np} = \frac{1}{H_t} \left( \frac{\delta_{ik}\delta_{jl} + \delta_{il}\delta_{jk}}{2} - \frac{\delta_{ij}\delta_{kl}}{\delta_{mn}\delta_{mn}} - \frac{s_{ij}S_{kl}}{s_{mn}S_{mn}} \right) \quad (17)$$

For the triaxial state where the third stress invariant is a constant (i.e., the Lode angle is  $30^\circ$  for triaxial compression and  $-30^\circ$  for triaxial tension), the compliance tensor  $C_{ijkl}^{np}$  has the following form:

$$C_{ijkl}^{np} = \frac{1}{H_t} \left( \frac{\delta_{ik}\delta_{jl} + \delta_{il}\delta_{jk}}{2} - \frac{\delta_{ij}\delta_{kl}}{3} - \frac{s_{ij}S_{kl}}{s_{mn}S_{mn}} \right) \quad (18)$$

For the plane strain state where all out-of-plane deformations are neglected and, for simplicity, the out-of-plane stresses are neglected as well, the compliance tensor  $C_{ijkl}^{np}$  takes the form as follows:

$$C_{ijkl}^{np} = \frac{1}{H_t} \left( \frac{\delta_{ik}\delta_{jl} + \delta_{il}\delta_{jk}}{2} - \frac{\delta_{ij}\delta_{kl}}{2} - \frac{s_{ij}S_{kl}}{s_{mn}S_{mn}} \right) \quad (19)$$

The stress rate,  $\hat{\sigma}_{kl}$ , can be determined by

$$\hat{\sigma}_{kl} = D_{klmn}^e \dot{\epsilon}_{mn} = D_{klmn}^e (\dot{\epsilon}_{mn} - \dot{\epsilon}_{mn}^{cp} - \dot{\epsilon}_{mn}^{np}) \quad (20)$$

where  $D_{klmn}^e$ =elastic stiffness tensor;  $\dot{\epsilon}_{mn}^e$ =elastic strain rate; and  $\dot{\epsilon}_{mn}$ =total strain rate.

Noting the following relations:

$$C_{ijkl}^{np} D_{klmn}^e = 2G C_{ijmn}^{np} \quad (21)$$

$$C_{ijmn}^{np} \dot{\epsilon}_{mn}^{cp} = 0 \quad (22)$$

$$C_{ijmn}^{np} \dot{\epsilon}_{mn}^{np} = \frac{1}{H_t} \dot{\epsilon}_{ij}^{np} \quad (23)$$

the noncoaxial plastic strain rate can be expressed in terms of  $C_{ijkl}^{np}$  as

$$\dot{\epsilon}_{ij}^{np} = \frac{2GH_t}{H_t + 2G} C_{ijmn}^{np} \dot{\epsilon}_{mn} \quad (24)$$

where  $G$ =elastic shear modulus.

On the other hand, the coaxial plastic strain rate can be expressed as

$$\dot{\epsilon}_{ij}^{cp} = \lambda \frac{\partial Q}{\partial \sigma_{ij}} = \frac{\partial Q}{\partial \sigma_{ij}} \frac{\frac{\partial F}{\partial \sigma_{st}} D_{stkl}^e \dot{\epsilon}_{kl}}{H_p + \frac{\partial F}{\partial \sigma_{st}} D_{stkl}^e \frac{\partial Q}{\partial \sigma_{kl}}} \quad (25)$$

where  $F=F(\sigma_{ij}, H)=0$  describes a general yield function; and  $H_p$  denotes the plastic hardening modulus.

Based on Eqs. (24) and (25), the total plastic strain rate is given as

$$\dot{\epsilon}_{ij}^p = \dot{\epsilon}_{ij}^{cp} + \dot{\epsilon}_{ij}^{np} = \left( \frac{\frac{\partial Q}{\partial \sigma_{ij}} \frac{\partial F}{\partial \sigma_{st}} D_{stkl}^e}{H_p + \frac{\partial F}{\partial \sigma_{st}} D_{stkl}^e \frac{\partial Q}{\partial \sigma_{kl}}} + \frac{2H_t G}{H_t + 2G} C_{ijkl}^{np} \right) \dot{\epsilon}_{kl} \quad (26)$$

The rate form of the stress-strain relationship is then formulated as

$$\begin{aligned} \hat{\sigma}_{ij} &= D_{ijkl}^{cp} \dot{\epsilon}_{kl} = D_{ijkl}^e (\dot{\epsilon}_{kl} - \dot{\epsilon}_{kl}^p) \\ &= \left( D_{ijkl}^e - \frac{D_{ijmn}^e \frac{\partial Q}{\partial \sigma_{mn}} \frac{\partial F}{\partial \sigma_{st}} D_{stkl}^e}{H_p + \frac{\partial F}{\partial \sigma_{st}} D_{stkl}^e \frac{\partial Q}{\partial \sigma_{kl}}} + \frac{2H_t G}{H_t + 2G} D_{ijmn}^e C_{mnlk}^{np} \right) \dot{\epsilon}_{kl} \end{aligned} \quad (27)$$

From Eq. (27), the elastic-plastic stiffness tensor incorporating noncoaxiality in the three-dimensional tensorial space can be derived as

$$D_{ijkl}^{ep} = D_{ijkl}^e - D_{ijmn}^e \left( \frac{\frac{\partial Q}{\partial \sigma_{mn}} \frac{\partial F}{\partial \sigma_{st}}}{H_p + \frac{\partial F}{\partial \sigma_{mn}} D_{mnst}^e \frac{\partial Q}{\partial \sigma_{st}}} + \frac{H_t}{H_t + 2G} C_{mnst}^{np} \right) D_{stkl}^e \quad (28)$$

The condition for the onset of the shear band is then determined as (Rice and Rudnicki 1980)

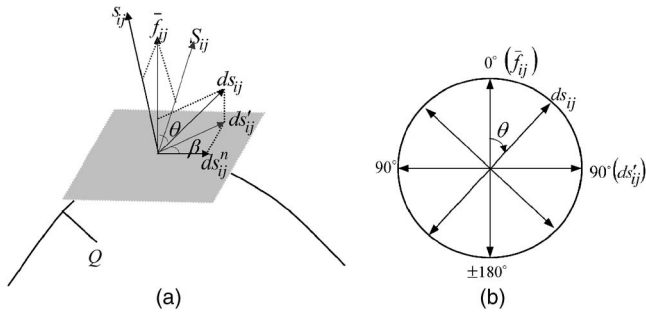


Fig. 2. Stress probe tests in three-dimensional deviatoric stress space

$$\det(A_{ik}(\mathbf{n})) = 0 \quad (29)$$

where  $A_{ik} = n_j D_{ijkl}^{ep} n_l - 1/2(\sigma_{ik} + \sigma_{jk} n_j n_i - \sigma_{ij} n_j n_k - \sigma_{jl} \delta_{ik} n_j n_l)$ ;  $\mathbf{n}$  (or  $n_i$ ) = vector normal to shear band; and  $D_{ijkl}^{ep}$  = elasto-plastic constitutive stiffness derived in Eq. (28).

### Stress Probe Tests of Noncoaxial Model

As an example, a three-dimensional coaxial, elasto-plastic model for frictional materials (Pietruszczak and Stolle 1987) is revised here in the proposed noncoaxial modeling framework to include the noncoaxiality effects. The yield function and plastic potential function are given as follows:

$$F = q - \eta \cdot g(\theta_\sigma) \cdot p = 0 \quad (30)$$

$$Q = q + \eta_c \cdot p \cdot g(\theta_\sigma) \cdot \ln\left(\frac{p}{p_0}\right) = 0 \quad (31)$$

where

$$q = \left(\frac{3}{2} s_{ij} s_{ij}\right)^{1/2}, \quad p = \frac{\sigma_{ii}}{3}, \quad \eta = \frac{q}{p} = \eta_f \frac{\varepsilon_s^{cp}}{A + \varepsilon_s^{cp}}$$

$$\eta_f = \frac{6 \sin \phi_f}{3 - \sin \phi_f}, \quad \varepsilon_s^{cp} = \int \dot{\varepsilon}_s^{cp} dt = \int \left(\frac{2}{3} \dot{e}_{ij}^{cp} \dot{e}_{ij}^{cp}\right)^{1/2} dt$$

$$g(\theta_\sigma) = \frac{(3 - \sin \phi)}{(3 - \sin \phi) + \sqrt{2} \sin \phi \sqrt{1 - \sin 3\theta_\sigma}} \left(-\frac{\pi}{6} \leq \theta_\sigma \leq \frac{\pi}{6}\right)$$

$$\theta_\sigma = \frac{1}{3} \sin^{-1} \left(-\frac{3\sqrt{3} J_3}{2 J_2^{3/2}}\right) \quad (32)$$

It is evident that  $\phi$  = mobilized friction angle;  $\phi_f$  = peak friction angle;  $\eta_c$  represents the value of  $\eta$  at  $\dot{\varepsilon}_{kk}^p = 0$ ;  $p_0$  = initial confining pressure; and  $A$  = material constant.

### Stress Probe Tests in Three-Dimensional Noncoaxial Stress Space

The stress probe tests in the three-dimensional noncoaxial deviatoric stress space are illustrated in Fig. 2. The tensor of the outward normal of the yield surface can be expressed as

$$\bar{f}_{ij} = \frac{\partial F(I_1, J_2, J_3)}{\partial s_{ij}} = b_1 s_{ij} + b_2 S_{ij} \quad (33)$$

where the coefficients  $b_1$  and  $b_2$  are analogous to  $a_1$  and  $a_2$  in Eq. (4).

The noncoaxiality between  $\bar{f}_{ij}$  and  $ds_{ij}$  (the stress increment) can be characterized using a deviation angle  $\theta$  defined as follows (Budiansky 1959)

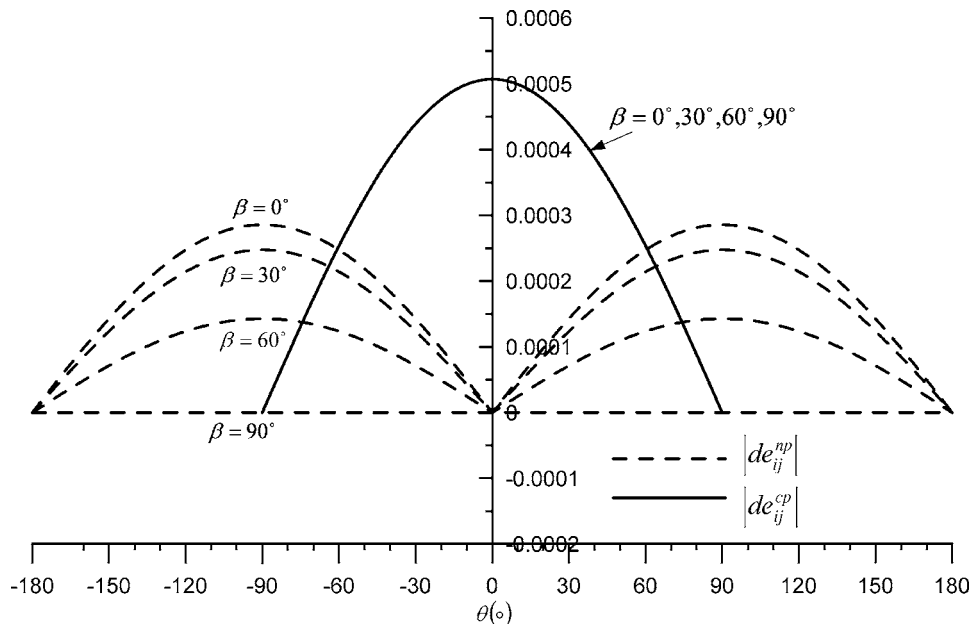


Fig. 3. Noncoaxial and coaxial deviatoric strains in probe tests

**Table 1.** Parameters for Three-Dimensional and Two-Dimensional Noncoaxial Models

Elastic parameters	Plastic parameters	
	Coaxial parameters	Noncoaxial parameters
$E=175$ MPa	$\eta_f = \begin{cases} 1.70 & \text{for 3D} \\ 0.66 & \text{for 2D} \end{cases}$	$H_t=2.5$ MPa
$\nu=0.1667$	$\eta_c = \begin{cases} 0.965 & \text{for 3D} \\ 0.36 & \text{for 2D} \end{cases}$	
	$A=0.001$	

$$\cos \theta = \frac{\bar{f}_{ij} ds_{ij}}{(\bar{f}_{kl} \bar{f}_{kl})^{1/2} (ds_{kl} ds_{kl})^{1/2}} \quad (34)$$

where  $\theta=0^\circ$  and  $\theta \neq 0^\circ$  represent coaxiality and noncoaxiality between  $\bar{f}_{ij}$  and  $ds_{ij}$ . The direction of  $ds_{ij}$  varies as  $\theta$  changes from  $-180$  to  $180^\circ$  in the noncoaxial plane  $ds_{ij}^n - \bar{f}_{ij}$  (Fig. 2).

Another parameter,  $\beta$ , defined as a deviation angle between  $ds_{ij}^n$  and the projective component of  $ds_{ij}$  on the yield surface, is introduced as follows:

$$\cos \beta = \frac{ds_{ij}' ds_{ij}^n}{(ds_{kl}' ds_{kl}')^{1/2} (ds_{kl}^n ds_{kl}^n)^{1/2}} \quad (35)$$

where

$$ds_{ij}' = ds_{ij} - \frac{\bar{f}_{kl} ds_{kl} \bar{f}_{ij}}{\bar{f}_{kl} \bar{f}_{kl}}$$

Now, assume that the initial stress state is isotropic with  $\sigma_{10}=\sigma_{20}=\sigma_{30}=200$  kPa. The probe tests are conducted in such a manner that  $\sigma_3$  is kept constant while  $\sigma_1$  and  $\sigma_2$  vary. The probe tests are started at the state of  $\sigma_1=900$  kPa and  $\sigma_2=210$  kPa. Given a small stress increment  $|ds_{ij}|=(ds_{kl} ds_{kl})^{1/2}=1.0$  kPa at this state, the incremental noncoaxial and coaxial plastic strains are computed and shown in Fig. 3 as a function of  $\theta$  and  $\beta$ . The model parameters used in the computation are given in Table 1. As will be described in the next section, these parameters are calibrated from the biaxial test results of Han and Drescher (1993) for Ottawa sand.

It can be seen that the noncoaxial strain always occurs under the condition of  $\theta \neq 0^\circ$  and  $\beta \neq 90^\circ$ , with the largest values occurring in the case of  $\beta=0^\circ$ . By comparison, the coaxial deviatoric strain is found to be independent of the angle  $\beta$ . If the effect of noncoaxiality is ignored, the stress-strain response will be totally elastic when the direction of the stress increment satisfies the condition  $\beta=90^\circ$  and  $\theta=90-180^\circ$  or  $\theta=-90--180^\circ$ .

### Deformation Localization Analysis

Compared to the triaxial and true triaxial tests, a more complete and clearer strain localization response can be observed in biaxial tests. A series of high-quality biaxial tests performed by Han and Drescher (1993) are used here as a benchmark. A bifurcation analysis for biaxial tests is traditionally conducted as a two-dimensional plane strain problem by ignoring the out-of-plane deformation. In addition to this traditional treatment, the problem will also be analyzed here as a three-dimensional problem by including the influence of the third stress invariant.

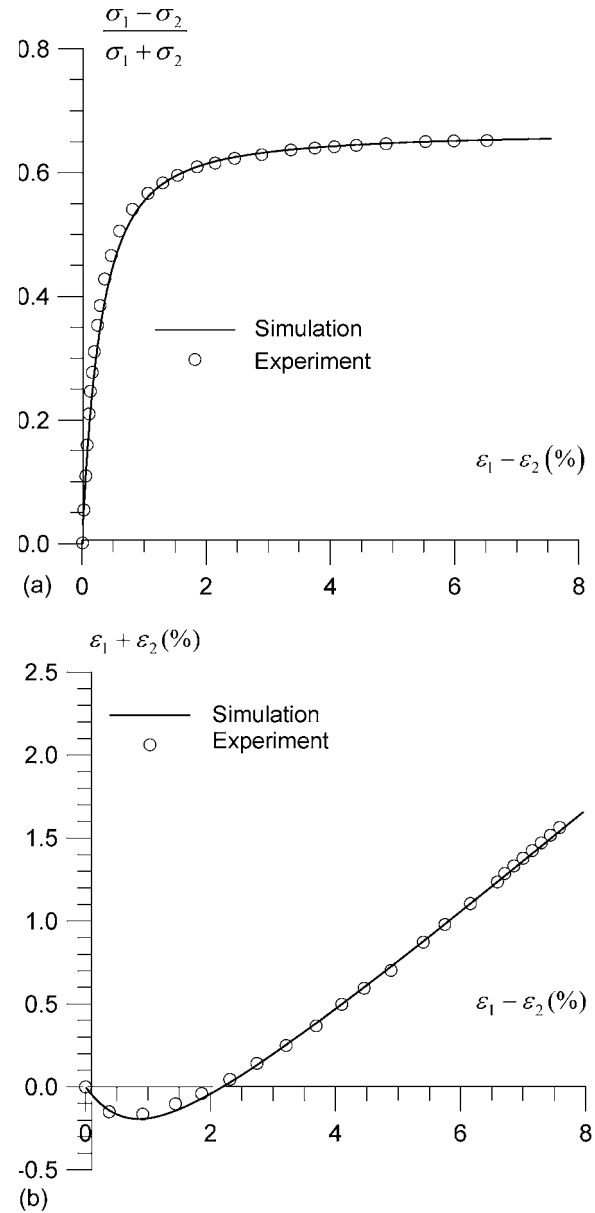


**Fig. 4.** Prebifurcation response at confining pressure of 200 kPa: (a) stress ratio versus shear strain; (b) volumetric strain versus shear strain

The test material used in Han and Drescher (1993) was coarse, poorly graded Ottawa sand with an initial void ratio between 0.32 and 0.33. All tests were performed under displacement controlled axial loading with the displacement rate of 0.2 mm/min. The specimens were subjected to initial confining pressures of 50, 100, 200, and 400 kPa, respectively. Typical experimental results at the confining pressure of 200 kPa are shown in Fig. 4. The prelocalization response is assumed to be the constitutive behavior in a homogeneous state. The model parameters,  $\eta_f$ ,  $\eta_c$ , and  $A$ , are calibrated using the prelocalization response. The elastic parameters  $E$  and  $\nu$  are directly obtained from Han and Drescher (1993). The noncoaxial parameter,  $H_t$ , which governs the incremental nonlinear response, is preferred to calibrate from the experiments with principal stress rotation. As there was no stress rotation test in Han and Drescher (1993),  $H_t$  is approximately estimated here by matching the bifurcation point in the case of

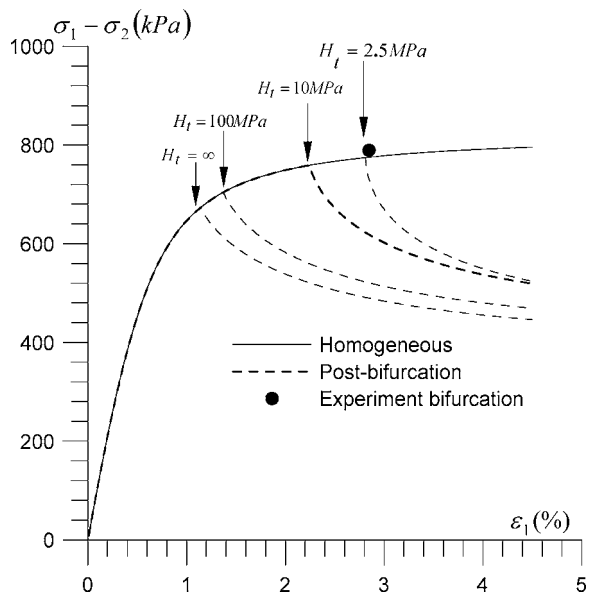


**Fig. 5.** Effect of plastic modulus on bifurcation ( $p_0=200$  kPa)

confining pressure of 200 kPa (Fig. 5). All model parameters are summarized in Table 1.

As shown in Fig. 5, the noncoaxial parameter  $H_t$  has a profound effect on the bifurcation state. The discrepancy between the prediction produced by the coaxial flow theory ( $H_t=\infty$ ) and the experimental observation is significant. However, when the value of  $H_t$  decreases, the occurrence of bifurcation is delayed and a reasonable agreement is obtained at  $H_t=2.5$  MPa.

Fig. 6 shows the shear deformation ( $\epsilon_1-\epsilon_2$ ) at bifurcation as affected by the plastic modulus,  $H_t$ . It is noted that in both the two-dimensional and three-dimensional noncoaxial modeling, the shear strain at bifurcation can be reasonably predicted by setting the plastic modulus to be 2.0–3.0 MPa. By defining  $(\epsilon_1-\epsilon_2)_{\max}$  as the predicted shear strain at bifurcation and  $H_{t(\max)}$  as the corresponding plastic modulus, it is of interest to examine the dependence of  $(\epsilon_1-\epsilon_2)_{\max}$  and  $H_{t(\max)}$  on the confining pressure. The results of analysis are shown in Figs. 7 and 8, indicating that both  $(\epsilon_1-\epsilon_2)_{\max}$  and  $H_{t(\max)}$  tend to increase with the initial confining pressure.

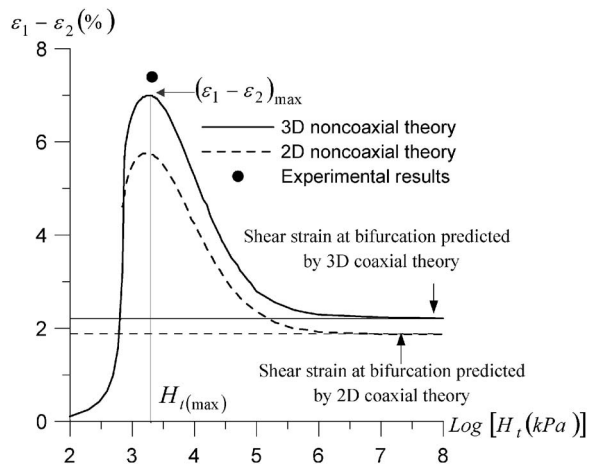


**Fig. 6.** Effect of plastic modulus on shear strain at bifurcation ( $p_0=200$  kPa)

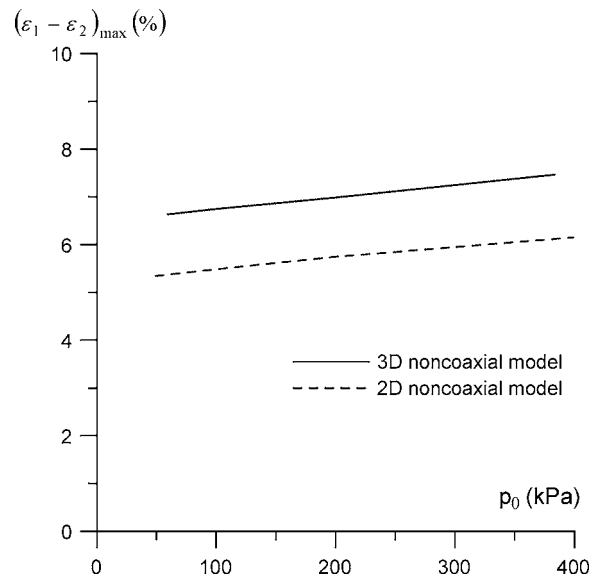


**Fig. 7.** Predicted shear strain  $(\epsilon_1-\epsilon_3)_{\max}$  versus confining pressure

Figs. 9–11 compare the predictions for shear band inclination angle, shear strain at bifurcation, and dilatancy at bifurcation, respectively, with the experimental observations. The experimental results indicate that the shear band orientation is dependent on the confining pressure: a higher confining pressure will give a smaller inclination angle. Clearly, the coaxial plasticity model fails to predict this trend; at a higher confining pressure it gives a greater inclination angle. Both the two-dimensional and three-dimensional noncoaxial models provide reasonably good predictions.

As for the shear strain at the initiation of shear band, the prediction produced by the three-dimensional noncoaxial model is the best, followed by the prediction of the two-dimensional noncoaxial model. The coaxial plasticity model gives the worst prediction. While all the models predict the general trend that the shear strain at the onset of shear band increases with increasing

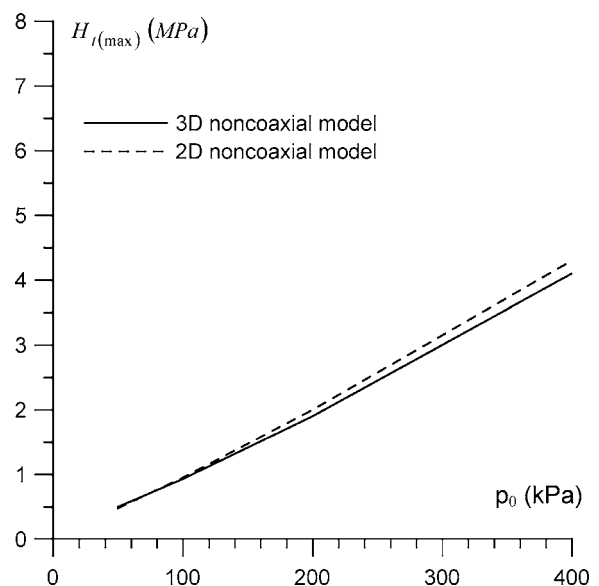


**Fig. 8.** Plastic modulus corresponding to  $(\epsilon_1-\epsilon_3)_{\max}$  versus confining pressure

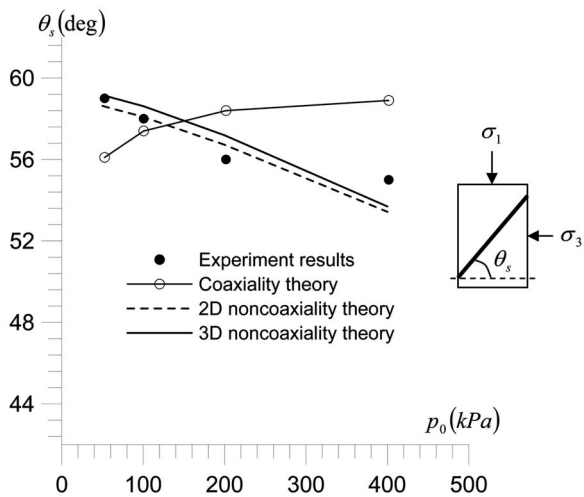


Fig. 9. Shear band inclination versus confining pressure

confining pressure, the noncoaxial plasticity models appear to give a slightly decreasing rate at large confining pressures. Compared to the noncoaxial models, the coaxial model predicts that the shear band initiates at a much smaller strain level throughout the range of confining pressures concerned.

The dilatancy in Fig. 11 is defined as  $(\dot{\epsilon}_1 - \dot{\epsilon}_2)/(\dot{\epsilon}_1 + \dot{\epsilon}_2)$ , with negative values for dilation and positive values for contraction. It is noted that the specimens always show dilatancy at the onset of shear band and the degree of dilation becomes small when the confining pressure increases. Again, the three-dimensional noncoaxial model provides the best prediction, whereas the coaxial model gives a poor prediction.

## Conclusions

Predicting the onset of shear band in geomaterials plays an important role in various geotechnical analyses involving stability problems. A traditional constitutive model implicitly assumes coaxiality between the principal directions of the stress and the rate

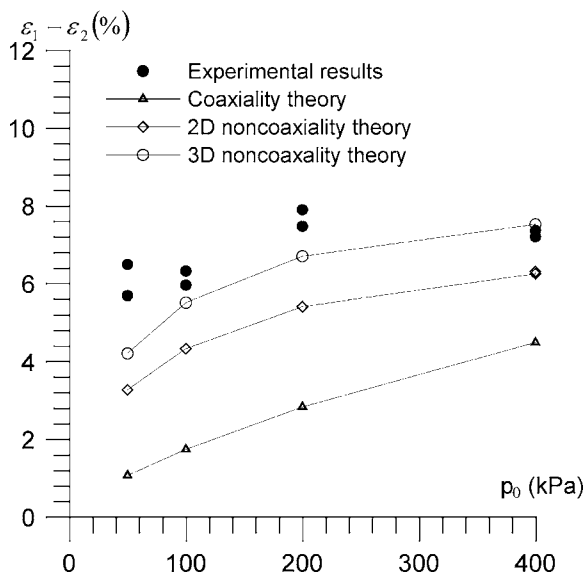


Fig. 10. Shear strain at bifurcation versus confining pressure

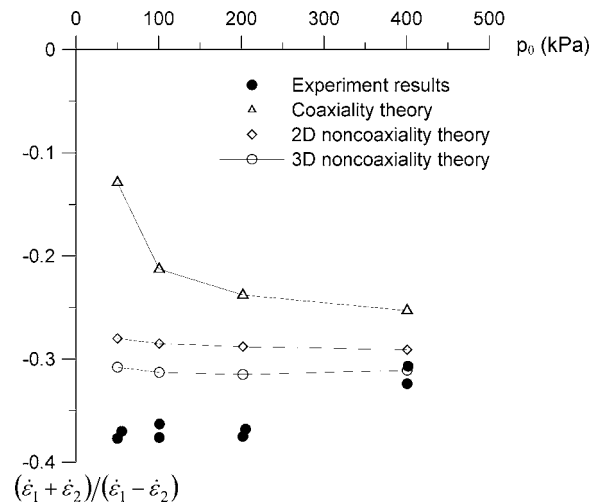


Fig. 11. Dilatancy at bifurcation versus confining pressure

of plastic deformation, which however contrasts with the accumulating experimental evidence of noncoaxiality. In this paper, a noncoaxial constitutive modeling platform has been established in the general three-dimensional stress space. It has been shown that the noncoaxial stress rate proposed by Rundnicki and Rice (1975) only represents the two-dimensional condition but not the three-dimensional condition.

A three-dimensional coaxial plasticity model has been revised within the proposed noncoaxial modeling framework to account for the effects of noncoaxiality. The performance of the three-dimensional noncoaxial plasticity model has been evaluated by comparison of its predictions with experimental observations and with those produced by the two-dimensional noncoaxial model and the coaxial plasticity model. The results show that, as compared to the two-dimensional noncoaxial model, the three-dimensional noncoaxial model can improve the predictions for the initiation and orientation of shear band as well as the dilatancy at the onset of shear band. The predictions produced by the coaxial plasticity model are generally poor however. The study also shows that the value of the plastic modulus,  $H_p$ , which governs the noncoaxial stress-strain response, can be identified as the one that gives a peak response of the deviatoric strain in the  $(\epsilon_1 - \epsilon_2)_{\max} - H_{t(\max)}$  plane.

While the theoretical developments presented here are limited to isotropic plasticity models, the framework may be extended to plasticity models with combined isotropic/kinematic hardening by introducing the back stress  $\bar{\sigma}_{ij} = \sigma_{ij} - \alpha_{ij}$ , where  $\alpha_{ij}$  = relative stress describing the translation of yield surface. A detailed discussion of this issue is beyond the scope of the paper and will be reported on in the future.

## Acknowledgments

The financial support provided by the National Natural Science Foundation of China (Grant Nos. 10402029 and 50179025), the Key Laboratory of Rock and Soil Mechanics of the Institute of Rock and Soil Mechanics, the Chinese Academy of Sciences (Grant No. Z110401), and the Research Grants Council of Hong Kong is acknowledged.

## Notation

The following symbols are used in the paper:

- $A$  = material constant;  
 $a_0, a_1, a_2$  = coefficients depending on stress invariants and plastic potential function;  
 $b_0, b_1, b_2$  = coefficients depending on stress invariants and yield function;  
 $C_{ijkl}^{np}$  = noncoaxial plastic tangential compliance tensor;  
 $D_{ijkl}^e$  = elastic tangential stiffness tensor;  
 $D_{ijkl}^{ep}$  = elasto-plastic tangential stiffness tensor;  
 $ds_{ij}$  = deviatoric stress increment;  
 $ds'_{ij}$  = projective component of  $ds_{ij}$  on yield surface;  
 $E$  = Young's modulus;  
 $\dot{\epsilon}_{ij}$  = deviatoric component of  $\dot{\epsilon}_{ij}$ ;  
 $e_0$  = initial void ratio;  
 $F$  = yield function;  
 $\bar{f}_{ij}$  = outward normal tensor of yield surface;  
 $G$  = shear modulus;  
 $H_t$  = tangential modulus governing noncoaxial response;  
 $I_1, J_2, J_3$  = stress invariants;  
 $Q$  = plastic potential function;  
 $S_{ij}$  = stress tensor independent of  $\delta_{ij}$  and  $s_{ij}$ ;  
 $s_{ij}$  = deviatoric stress;  
 $\beta$  = deviation angle between  $ds_{ij}^n$  and  $ds'_{ij}$ ;  
 $\delta_{ij}$  = Kronecker delta;  
 $\dot{\epsilon}_{ij}$  = rate of strain tensor;  
 $\eta$  = stress ratio;  
 $\eta_c$  = stress ratio at  $\epsilon_{kk}^p=0$ ;  
 $\eta_f$  = stress ratio at peak/failure;  
 $\theta$  = deviation angle between  $\bar{f}_{ij}$  and  $ds_{ij}$ ;  
 $\lambda$  = nonnegative scalar that varies throughout plastic loading history;  
 $\nu$  = Poisson's ratio;  
 $\sigma_{ij}$  = Cauchy stress;  
 $\dot{\sigma}_{ij}(\dot{\sigma}_{ij})$  = rate of Cauchy (Jaumann) stress;  
 $\phi$  = mobilized friction angle;  
 $\phi_f$  = peak friction angle;  
 $(\dot{\quad})$  = rate of tensor (or vector);  
 $(\quad)^{cp}$  = coaxial plastic component of tensor;  
 $(\quad)^e$  = elastic component of tensor;  
 $(\quad)^{np}$  = noncoaxial plastic component of tensor;  
 $(\quad)^p$  = plastic component of tensor; and  
 $|(\quad)|$  = magnitude of tensor.

## References

Alshibli, K. A., Batiste, S. N., and Sture, S. (2003). "Strain localization in sand: plane strain versus triaxial compression." *J. Geotech. Geoenviron. Eng.*, 129(6), 483–494.

- Arthur, J. R. F., Chua, K. S., and Dunstan, T. (1977). "Induced anisotropy in a sand." *Geotechnique*, 27(1), 613–622.
- Bardet, J. P. (1991). "A comprehensive review of strain localization in elastoplastic soils." *Comput. Geotech.*, 11, 163–188.
- Budiansky, B. (1959). "A reassessment of deformation theories of plasticity." *J. Appl. Mech.*, 26, 259–264.
- Chu, J., Lo, S. C. R., and Lee, I. K. (1996). "Strain softening and shear band formation of sand in multi-axial testing." *Geotechnique*, 46(1), 63–82.
- Desrues, J., Lanier, J., and Stutz, P. (1985). "Localization of the deformation in tests on sand sample." *Eng. Fract. Mech.*, 21(4), 909–921.
- Gutierrez, M., Ishihara, K., and Towhata, I. (1991). "Flow theory for sand during rotation of principal stress direction." *Soils Found.*, 31(4), 121–132.
- Hammad, W. (1991). "Modélisation non linéaire et étude expérimentale des bandes de cisaillement dans les sables." Thèse de Doctorat, l'Univ. J. Fourier, Grenoble, France.
- Han, C., and Drescher, A. (1993). "Shear bands in biaxial tests on dry coarse sand." *Soils Found.*, 33(1), 118–132.
- Ishihara, K., and Towhata, I. (1983). "Sand response to cyclic rotation of principal stress directions as induced by wave loads." *Soils Found.*, 23(4), 11–26.
- Mooney, M. A., Finno, R. J., and Viggiani, M. G. (1998). "A unique critical state for sand?" *J. Geotech. Geoenviron. Eng.*, 124(11), 1100–1108.
- Ottosen, N. S., and Runesson, K. (1991). "Properties of discontinuous bifurcations in elasto-plasticity." *Int. J. Solids Struct.*, 27(4), 401–421.
- Papamichos, E., and Vardoulakis, I. (1995). "Shear band formation in sand according to noncoaxial plasticity model." *Geotechnique*, 45(4), 649–661.
- Pietruszczak, S., and Stolle, D. F. E. (1987). "Modelling of sand behavior under earthquake excitation." *Int. J. Numer. Analyt. Meth. Geomech.*, 11, 221–240.
- Pradel, D., Ishihara, K., and Gutierrez, M. (1990). "Yielding and flow of sand under principal axes rotation." *Soils Found.*, 30(1), 87–89.
- Rice, J. R., and Rudnicki, J. W. (1980). "A note on some features of theory of the localization of deformation." *Int. J. Solids Struct.*, 16, 507–605.
- Rudnicki, J. W., and Rice, J. R. (1975). "Conditions for the localization of the deformation in pressure sensitive dilatant materials." *J. Mech. Phys. Solids*, 23, 371–394.
- Vardoulakis, I. (1980). "Shear band inclination and shear modulus of sand in biaxial tests." *Int. J. Numer. Analyt. Meth. Geomech.*, 4, 103–119.
- Vardoulakis, I., and Graf, B. (1985). "Calibration of constitutive models for granular materials using data from biaxial experiments." *Geotechnique*, 35(3), 299–317.
- Vermeer, P. A. (1982). "A simple shear band analysis using compliances." *Proc., IUTAM Conf. on Deformation and Failure of Granular Materials*, Balkema, Rotterdam, The Netherlands, 439–499.
- Wang, Q., and Lade, P. V. (2001). "Shear banding in true triaxial tests and its effect on failure in sand." *J. Eng. Mech.*, 127(8), 754–761.
- Yamamoto, J. A., and Shapiro, S. (2002). "Failure and shear band in three-dimensional experiments on loose silty sands." *Proc., 15th Engineering Mechanics Conf.*, ASCE, Reston, Va.
- Yang, Z. X., Li, X. S., and Yang, J. (2007). "Undrained anisotropy and rotational shear in granular soil." *Geotechnique*, 57(4), 371–384.